Bull. Mater. Sci., Vol. 37, No. 2, April 2014, pp. 309–314. © Indian Academy of Sciences.

Preparation and characterization of PEG–$Mg(CH_3COO)_2$–CeO_2 composite polymer electrolytes for battery application

ANJI REDDY POLU* **and RANVEER KUMAR†**
Department of Physics, K L University, Guntur 522 502, India
†Department of Physics, Dr. H S Gour University (A Central University), Sagar 470 003, India

MS received 13 June 2012; revised 19 February 2013

Abstract. Composite polymer electrolytes based on poly(ethylene glycol) (PEG), magnesium acetate [$Mg(CH_3COO)_2$], and x wt% of cerium oxide (CeO_2) ceramic fillers (where x = 0, 5, 10, 15 and 20, respectively) have been prepared using solution casting technique. X-ray diffraction patterns of PEG–$Mg(CH_3COO)_2$ with CeO_2 ceramic filler indicated the decrease in the degree of crystallinity with increasing concentration of the filler. DSC measurements of PEG–$Mg(CH_3COO)_2$–CeO_2 composite polymer electrolyte system showed that the melting temperature is shifted towards the lower temperature with increase of the filler concentration. The conductivity results indicate that the incorporation of ceramic filler up to a certain concentration (i.e. 15 wt%) increases the ionic conductivity and upon further addition the conductivity decreases. The transference number data indicated the dominance of ion-type charge transport in these specimens. Using this (PEG–$Mg(CH_3COO)_2$–CeO_2) (85-15-15) electrolyte, solid-state electrochemical cell was fabricated and their discharge profiles were studied under a constant load of 100 kΩ.

Keywords. **Polymer electrolyte; poly(ethylene glycol); ceramic filler; transference number; electrochemical cell.**

1. Introduction

Polymer electrolytes are becoming increasingly important because of their potential use in several electrochemical devices: 'smart' windows, displays, sensors and more importantly, rechargeable solid-state lithium batteries. Their high energy densities combined with the potential for low-cost manufacturing technologies render solid-state batteries with polymer electrolytes extremely attractive for the usage of portable consumer electronics products. Compared to liquid electrolytes, solid polymer electrolytes would eliminate electrolyte leakage, limit electrolyte–electrode reactions and allow tremendous flexibility in design. An excellent candidate for anode material is magnesium, which is an active metal and easily obtained in the earth's crust. In addition, the natural abundance of magnesium makes magnesium-based devices cheaper than those based on lithium. Moreover, magnesium is less reactive than lithium towards oxygen and humid atmospheres minimizing hazards in open air. It is a non-toxic and environmental friendly element, whose ionic radii is comparable with that of lithium meaning that magnesium batteries may use insertion compounds that have been proposed for lithium cells. Magnesium has been successfully employed as anode in the primary and reserve batteries (Robinson 1976). About 22 years ago Gregory group (Gregory *et al* 1990) reported the electrochemical reversible deposition and dissolution process of magnesium in $Mg(BPh_2Bu_2)_2$, where, Ph and Bu are phenyl and butyl groups, respectively. Hence, it seems that the development of rechargeable batteries could be a realistic goal. Possibility of using the simple salt solutions in aprotic solutions is impractical due to the passivation phenomena, which hinders Mg^{2+} ions during the charging and discharging.

Composite polymer electrolytes (CPEs) comprising of a polymer host, doping salt and inorganic/ceramic filler were first demonstrated by Weston and Steele in 1982 (Weston and Steele 1982). The addition of fillers into the polymer matrices improves both the mechanical strength of the polymer (Weston and Steele 1982; Cho and Liu 1997) and their ionic conductivities (Wieczorek *et al* 1989; Croce and Scrosati 1993; Peled *et al* 1995). The additives used include SiO_2 (Matsuo and Kuwano 1995; Sekhon and Sandhar 1998; Capiglia *et al* 1999), ZrO_2 (Rajendran and Uma 2000a, b), TiO_2 (Polu and Kumar 2011), $LiAlO_2$ (Morita *et al* 2001), CeO_2 (Vijayakumar *et al* 2008), Al_2O_3 (Groce *et al* 2001) etc. and in most work on composite polymer electrolytes, the electrolyte is usually based on high molecular weight PEO (Wieczorek *et al* 1995; Sekhon and Sandhar 1998; Capiglia *et al* 1999; Morita *et al* 2001; Vijayakumar *et al* 2008; Polu and Kumar 2011). Little attention has been paid to the somewhat low molecular weight polymers. Bearing these facts in mind, we have prepared and published our previous work with poly(ethylene glycol) (PEG) of molecular weight 4000, complexed with $Mg(CH_3COO)_2$ salt (Polu *et al* 2011).

In this study, we report the composite solid polymer electrolytes prepared by the addition of CeO_2 particles to PEG–$Mg(CH_3COO)_2$. The purpose of this study is

*Author for correspondence (reddyphysics06@gmail.com)

to emphasize the extraordinary effect occurring in PEG–$Mg(CH_3COO)_2$–CeO_2 composite polymer electrolytes. Our results demonstrate that the dispersion of CeO_2 particles in PEG–$Mg(CH_3COO)_2$ matrix leads to an increase in the ionic conductivity of the composite polymer electrolytes. The resultant electrolyte films have been characterized by XRD and DSC analyses. The conductivity of the polymer electrolytes is measured using a.c. impedance technique in the temperature range 303–333 K.

2. Experimental

PEG (average molecular weight 4,000) purchased from CDH, India, was dried at 40 °C for 5 h; $Mg(CH_3COO)_2$ (CDH, India) was also dried at 40 °C for 24 h and CeO_2 procured from LOBA Chemie, of particle size < 5 μm was used. Solid polymer electrolyte samples were prepared using the solution cast technique. PEG (molecular weight of 4,000) was used as the polymer. $Mg(CH_3COO)_2$ was added accordingly. The solvent used in this work is distilled water. The mixture was stirred up to 10 h to obtain a homogeneous solution. After incorporating the required amount of inorganic filler (CeO_2 powder) was suspended in the solution and stirred for about 10 h. The solution was then poured into the glass petridishes and evaporated slowly at room temperature under vaccum. The polymer electrolyte samples were then transferred into a desiccator for further drying before the test.

In order to investigate the nature of these polymer electrolyte films, WAXD patterns were recorded in the diffraction angular 2θ range of 10–70° by a Philips X'Pert PRO (Almelo, The Netherlands) diffractometer, working in the reflection geometry and equipped with a graphite monochromator on the diffracted beam (CuKα radiation). The thermal response was studied by differential scanning calorimetry (TA Instruments model 2920 calorimeter) in the static nitrogen atmosphere at a heating rate of 5 °C/min in the temperature range of 0–100 °C. Impedance measurements were carried out in the temperature range 303–333 K using HIOKI 3532-50 LCR Hitester over a frequency range of 42 Hz to 5 MHz. The transference number measurements were made using Wagner's polarization technique (Wagner and Wagner 1957). Solid-state electrochemical cells were fabricated in the configuration Mg/(PEG–$Mg(CH_3COO)_2$–CeO_2)/(I_2 + C + electrolyte). The discharge characteristics of the cells were monitored under a constant load of 100 kΩ.

3. Results and discussion

Figure 1 shows X-ray diffraction patterns for 85PEG–15$Mg(CH_3COO)_2$ polymer electrolyte with x wt% of CeO_2 (x = 0, 5, 10, 15, 20) and pure CeO_2. X-ray diffraction analysis shows the decrease of crystallinity of the composite polymer electrolytes in comparison to the electrolyte without CeO_2. The intensities of crystalline peak of PEG in the vicinity of 19·2 and 23·4° has decreased remarkably according to the amount of cerium oxide introduced into the polymer electrolyte. In other words, volume fraction of amorphous phase in PEG polymer electrolyte increased with the amount of cerium oxide into the polymer matrix. For composite polymer electrolyte membranes, the peak intensity is decreased with increase in CeO_2 content up to 15 wt% which indicates the amorphous structure of the electrolyte membrane. Above 15 wt% of CeO_2 content, the peak intensity again enhanced suggesting an increase in the degree of crystallinity. Increased amorphousness in the composite polymer electrolyte membrane, which gives rise to higher conductivity is attributed to addition of the filler. Dispersed phase submicron size filler particles prevent the polymer chain reorganization, resulting in reduction in polymer crystallinity which gives rise to an increase in ionic conductivity (Croce *et al* 1998).

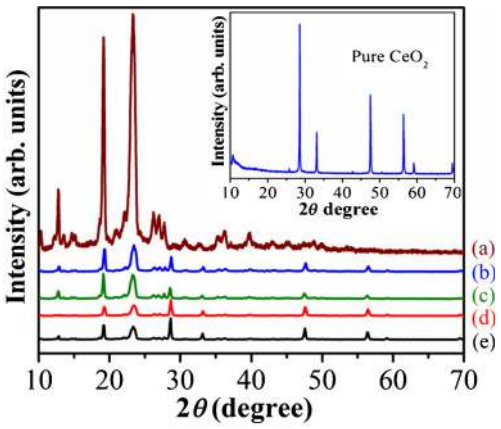

Figure 1. X-ray diffraction patterns of pure CeO_2 and (PEG–$Mg(CH_3COO)_2$–CeO_2) CPEs, (a) 85-15-0, (b) 85-15-05, (c) 85-15-10, (d) 85-15-15 and (e) 85-15-20.

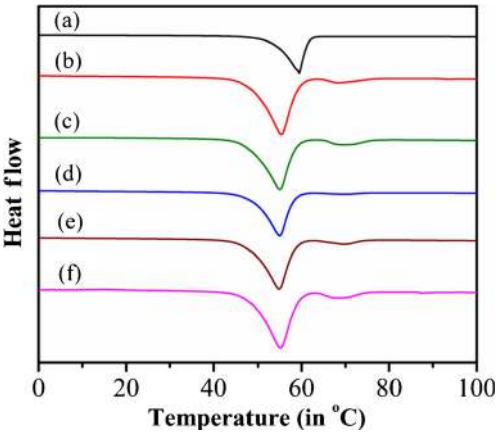

Figure 2. DSC curves of (a) pure PEG and (PEG–$Mg(CH_3COO)_2$–CeO_2) CPEs, (b) 85-15-0, (c) 85-15-05, (d) 85-15-10, (e) 85-15-15 and (f) 85-15-20.

Figure 2 shows DSC curves of pure PEG and 85PEG–15$Mg(CH_3COO)_2$ polymer electrolyte with x wt% CeO_2

($x = 0, 5, 10, 15, 20$) in the temperature range of 0–100 °C. There is a characteristic endothermic peak in the order of 54–56 °C, which is attributed to the melting point of crystalline PEG. The melting point of PEG of CPE is a little lower than the polymer electrolyte without cerium oxide. This phenomenon may be due to the local structural changes by disorder arrangement of lamellar structure when cerium oxide powders are introduced into polymer matrix. By assuming pure PEG was 100% crystalline, the relative percentage of crystallinity (X_c) was calculated based on the following equation with DSC data.

$$X_c = \left(\Delta H_m / \Delta H_m^0\right) \times 100\%, \quad (1)$$

where ΔH_m^0 is the standard enthalpy of fusion of pure PEG, 204·3 J/g and ΔH_m the enthalpy of fusion of the composite polymer electrolyte. X_c, ΔH_m and the crystalline melting temperature (T_m) for all CPE membranes are presented in table 1. From table 1 and figure 2, it is clear that melting temperature (T_m) and crystallinity (X_c) are decreasing with the addition of CeO_2 content up to 15 wt% and then slightly increases in the electrolyte membranes.

The reorganization of polymer chain may hinder by the cross-linking centres formed by the interaction of the Lewis-acid groups of filler with the polar groups of polymer. As a result, the degree of crystallization of polymer matrix decreases with the addition of filler (Ash *et al* 2002). Addition of CeO_2 in the polymer electrolytes is more responsible to the segmental chain motion of the polymer. In addition, above 15 wt% of CeO_2 in PEG matrix results in an increase in T_m, ΔH_m and X_c. It is ascribed to the increase of CeO_2 content above 15 wt% in the polymer matrix causes aggregation of particles which increase the crystallinity of CPE membrane. This leads to lower segmental mobility and hence reduced ionic conductivity.

Impedance spectroscopy is a relatively new and powerful method of characterizing many of the electrical properties of electrolyte materials and their interfaces with electronically conducting electrodes. Impedance plot (plot between real and imaginary parts of impedance) for 85PEG–15Mg(CH$_3$COO)$_2$–15 wt% of CeO_2 polymer composite at different temperatures is shown in figure 3.

The typical Nyquist plot of the samples comprises of a broadened semicircle in the high frequency region followed by a tail (spike) in the lower frequency region. The higher frequency semicircle can be ascribed mainly to the bulk properties of the materials, where as the low frequency spike indicates the presence of double layer capacitance at the electrode/sample interface (Macdonald 1987). The intercept of the semicircle with the real axis (Z') at low frequency (end) give rise to the bulk (ionic) resistance (R_b) of the materials. It can be observed from the plots that as the temperature increases, the diameter of the semicircle at higher frequency decreases, implying that the bulk resistance (R_b) decreases. By knowing the bulk resistance (R_b) along with the dimensions of the sample, the conductivity of the sample has been calculated by using the equation:

$$\sigma = L / R_b A, \quad (2)$$

where L and A are the thickness and area of the polymer electrolyte samples, respectively.

Figure 4 shows variation of conductivity with CeO_2 concentration at 303 K. The conductivity increases with the concentration of CeO_2 and shows a maximum value of $3{\cdot}40 \times 10^{-6}$ Scm^{-1} for 15 wt% of CeO_2 to PEG–Mg(CH$_3$COO)$_2$ polymer complex. The conductivity decreases with increasing concentration of CeO_2 (above 15 wt%). The conductivity of 85PEG–15Mg(CH$_3$COO)$_2$ polymer electrolyte system without CeO_2 is found to be $1{\cdot}07 \times 10^{-6}$ Scm^{-1} at 303 K (Polu *et al* 2011). The enhancement of ionic conductivity is expected due to the addition of CeO_2 which interacts with either/or both the anion and cation thereby

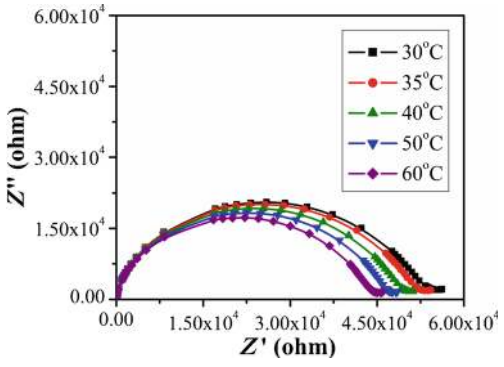

Figure 3. Complex impedance plots for (PEG–Mg(CH$_3$COO)$_2$–CeO$_2$) (85-15-15) composite polymer electrolyte at different temperatures.

Table 1. DSC results.

Sample	CeO$_2$ concentration (in wt%)	Melting point (T_m) (in °C)	ΔH_m (J/g)	X_c (in %)
Pure PEG		59·42	204·3	100
85PEG–15Mg(CH$_3$COO)$_2$	0	55·32	185·0	90·6
85PEG–15Mg(CH$_3$COO)$_2$	5	54·96	162·8	79·7
85PEG–15Mg(CH$_3$COO)$_2$	10	54·48	153·4	75·1
85PEG–15Mg(CH$_3$COO)$_2$	15	54·06	148·2	72·5
85PEG–15Mg(CH$_3$COO)$_2$	20	55·08	170·5	83·5

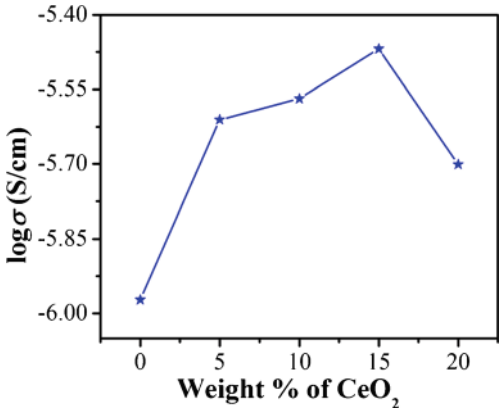

Figure 4. Effect of the concentration of CeO_2 on the conductivity of 85PEG–15Mg$(CH_3COO)_2$ polymer electrolyte at room temperature (303 K).

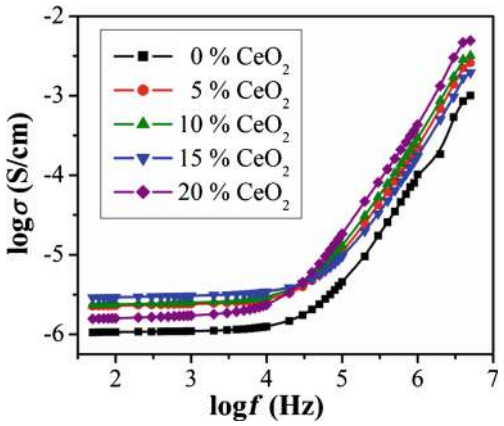

Figure 5. Conductance spectra of 85PEG–15Mg$(CH_3COO)_2$-x wt% of CeO_2 (x = 0, 5, 10, 15, 20) composite polymer electrolytes.

reducing ion pairing and increases the number of charge carriers. A reduction in softening point (and also the glass transition temperature, T_g) of polymers upon addition of fine ceramic particles has been demonstrated by several groups (Przyluski and Wieczorek 1989). The increase in conductivity has been attributed to (i) the ceramic particles acting as nucleation centres in the formation of minute crystallites (Wieczorek 1992; Chandra *et al* 1995); (ii) the ceramic particles aiding in the formation of amorphous phases in the polymer electrolyte (Plocharski *et al* 1989; Munichandraiah *et al* 1995) and (iii) to the formation of a new kinetic path via polymer ceramic boundaries (Kumar and Scanlon 1994; Przyluski *et al* 1995). Irrespective of the reasoning, it can be safely assumed that as T_g decreases, the amorphous phase or the less-ordered regions become more flexible resulting in the increased segmental motion of the polymer chains as reflected by enhanced conductivity (Choi *et al* 1997). However, the conductivity does not continue to rise indefinitely, with increasing concentration of CeO_2. In fact, it falls once when an optimum concentration of CeO_2 is crossed. This behaviour is a direct consequence of high concentrations of the ceramic filler, which leads to well-defined crystallite regions. Further, beyond this optimum concentration, CeO_2 particles tend to impede ionic movement by acting as mere insulators.

The frequency dependent a.c. conductivity of PEG–Mg$(CH_3COO)_2$ + x wt% of CeO_2 for different values of x at room temperature (303 K) is shown in figure 5. The a.c. conductivity patterns show a frequency independent plateau in the low frequency region and exhibits dispersion at higher frequencies. The frequency dependent conductivity in composite polymer electrolyte seems to follow the well known universal power law (Jonscher 1977). The effect of electrode polarization is evidenced by small deviation from σ_{dc} (plateau region) value in the conductivity spectrum (in the low frequency region). It has been observed that the maximum value of d.c. conductivity was found to be 3·44 × 10^{-6} Scm^{-1} for 15 wt% of CeO_2 concentration whereas

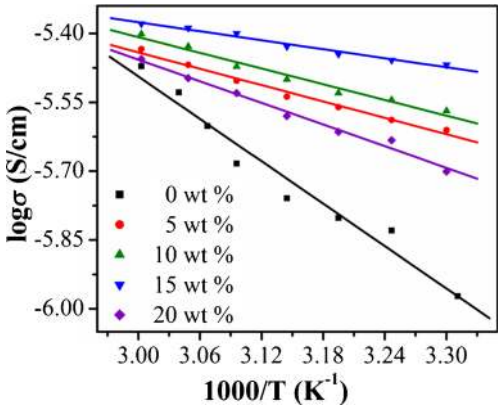

Figure 6. Temperature dependent conductivity of 85PEG–15Mg$(CH_3COO)_2$-x wt% of CeO_2 (x = 0, 5, 10, 15, 20) composite polymer electrolytes.

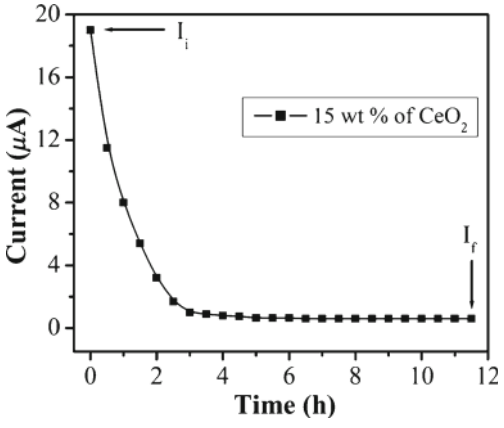

Figure 7. Polarization current vs time plot of (PEG–Mg$(CH_3COO)_2$–CeO_2) (85-15-15) electrolyte film.

for higher CeO_2 concentration, the conductivity decreases monotonically (room temperature). This observation can be explained by an empirical (3):

$$\sigma = \Sigma n_i \mu_i z_i, \tag{3}$$

where n_i, μ_i and z_i refer to charge carrier, ionic mobility and ionic charge of ith ion, respectively. It is clear from the equation that the conductivity depends on the amount of charge carrier (n_i) and the mobility of the ionic species in the system. Addition of ceramic filler can increase the fraction of free ions (i.e. increase of n_i) because the negative charge in CeO_2 fillers can interact with Mg^{2+} cation and disturb the attractive forces between cation and anion of the salt. When excess amount of CeO_2 is added to polymer–salt complex, there may be an increase in the system viscosity and thus restricts the cation mobility (i.e. decrease of μ_i), as a result, lower ionic conductivity is observed. Therefore, it can be concluded that the addition of optimum filler concentration (i.e. 15 wt% of CeO_2) provides the most suitable environment for the ionic transport in achieving the highest conductivity.

Figure 6 shows conductivity ($\log\sigma$) vs temperature inverse plots of PEG–$Mg(CH_3COO)_2$–CeO_2 composite-polymer electrolyte system with varying the filler concentration. From figure 6, it is observed that the conductivity vs temperature behaviour of the system is linear, i.e. follows Arrhenius relationship

$$\sigma = \sigma_0 \exp(-E_a/kT), \tag{4}$$

where σ_0 is the pre-exponential factor, E_a the activation energy and k the Boltzmann constant.

The behaviour of conductivity enhancement with temperature can be understood in terms of the free-volume model (Rajendran and Uma 2000a, b). As the temperature increases, the polymer can expand easily and produce free volume. Thus, as temperature increases, the free volume also increases. The resulting conductivity, represented by the overall mobility of ions and the polymer, is determined by the free volume around the polymer chains. Therefore, as temperature increases, ions, solvated molecules or polymer segments can move into the free volume. This leads to an increase in ion mobility and segmental mobility that will assist ion transport and virtually compensate for the retarding effect of the ion clouds.

The ionic transference number of the mobile species in the polymer electrolyte was calculated by Wagner's d.c. polarization technique (Wagner and Wagner 1957). This method was used to analyse the mobile species in the electrolyte. The polarization current was monitored as a function of time on the application of d.c. potential (1·5 V) across the cell in the configuration Mg/(PEG–$Mg(CH_3COO)_2$–CeO_2) (85-15-15)/C is shown in figure 7. The current decays immediately and asymptotically approaches steady state. The total ionic transference number was calculated from the polarization current vs time plots using the standard equation:

$$t_{ion} = 1 - I_f/I_i, \tag{5}$$

$$t_{ele} = 1 - t_{ion}, \tag{6}$$

where I_i is the initial current and I_f the final residual current. The total ionic transference number was found to be ~0·97 in this polymer electrolyte system. This suggests that the charge transport in these polymer electrolytes is predominantly due to ions.

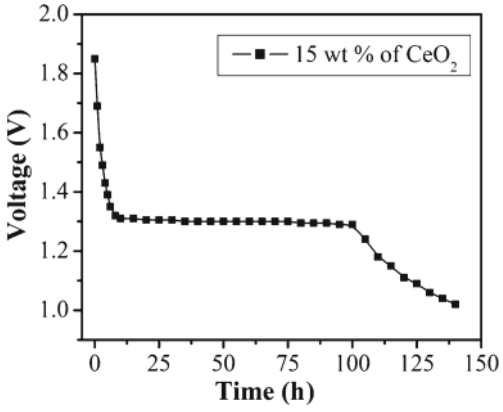

Figure 8. Discharge characteristic plot of (PEG–$Mg(CH_3COO)_2$–CeO_2) (85-15-15) electrochemical cell for a constant load of 100 kΩ.

Table 2. Comparison of present cell parameters with the data of other cells reported earlier.

Solid-state electrochemical cell configuration	Open circuit voltage (OCV) V	Discharge time for plateau region (h)	Reference
$Ag/(PVP + AgNO_3)/(I_2 + C + \text{electrolyte})$	0·46	82	Jaipal Reddy *et al* (1995)
$K/(PVP + PVA + KBrO_3)/(I_2 + C + \text{electrolyte})$	2·30	72	Subba Reddy *et al* (2004)
$Na/(PEO + NaYF4)/(I_2 + C + \text{electrolyte})$	2·45	96	Sreepathi Rao *et al* (1995)
$Mg/(PEO + Mg(NO_3)_2)/(I_2 + C + \text{electrolyte})$	1·85	142	Ramalingaiah *et al* (1996)
$Mg/(PEG + Mg(CH_3COO)_2)/(I_2 + C + \text{electrolyte})$	1·84	82	Polu and Kumar (2012)
$Mg/(PVA + Mg(CH_3COO)_2)/(I_2 + C + \text{electrolyte})$	1·84	87	Polu and Kumar (2012)
$Mg/(PVA + PEG + Mg(NO_3)_2)/(I_2 + C + \text{electrolyte})$	1·85	120	Polu *et al* (2012)
$Mg/(PEG + Mg(CH_3COO)_2 + CeO_2)/(I_2 + C + \text{electrolyte})$	1·85	90	Present

The discharge characteristics of the cell Mg/(PEG–$Mg(CH_3COO)_2$–CeO_2) $(85-15-15)/(I_2+C+$ electrolyte) at an ambient temperature for a constant load of 100 kΩ are shown in figure 8. The initial sharp decrease in voltage of these cells may be due to polarization and/or formation of a thin layer of magnesium salt at the electrode–electrolyte interface. Various cell parameters obtained for the cell are: open circuit voltage (OCV) = 1·85 V, cell weight = 1·84 g, area of the cell = 1·33 cm^2, discharge time for plateau region = 90 h, current density = 13·91 $\mu A/cm^2$, discharge capacity = 1·665 m A h, power density = 13·07 mW/kg and energy density = 1830 mW h/kg. The cell parameters for a number of solid-state cells reported earlier are given in table 2 along with the data of present cell. From table 2, it is clear that the cell parameters of the present electrolyte system is comparable with the cell parameters reported for other cells, thus offering an interesting option of application of these electrolytes for solid-state batteries.

4. Conclusions

The polymer electrolytes PEG–$Mg(CH_3COO)_2$ with different compositions of CeO_2 have been prepared by solution cast technique. Reduction in crystallinity and interaction with the polymer are established from XRD results after the addition of CeO_2. A decrease in melting temperature and percentage of crystallinity were observed on doping with filler in SPE. The maximum value of conductivity obtained is $3{\cdot}40 \times 10^{-6}$ Scm^{-1} for sample with 15 wt% of CeO_2 to PEG–$Mg(CH_3COO)_2$ polymer electrolyte system. The ionic transport number data in PEG–$Mg(CH_3COO)_2$–CeO_2 polymeric electrolyte films indicate that the conduction is predominantly due to ions. The cell parameters evaluated for the present cell are comparable with the cell parameters of earlier reported cells, thus offering an interesting option of application of these electrolytes for solid-state batteries.

References

Ash B J, Schadler L S and Siegel R W 2002 *Mater. Lett.* **55** 83

Capiglia C, Mustarelli P, Quartarone E, Tomassi C and Magistris A 1999 *Solid State Ionics* **118** 73

Chandra A, Srivastava P C and Chandra S 1995 *J. Mater. Sci.* **30** 3633

Cho J and Liu M 1997 *Electrochim. Acta* **42** 1481

Choi B K, Kim Y W and Shin K H 1997 *J. Power Sources* **68** 357

Croce F, Appetecchi G B, Persi L and Scrosati B 1998 *Nature* **394** 456

Croce F and Scrosati B 1993 *J. Power Sources* **43** 9

Gregory T D, Hoffman R J and Winterton R C 1990 *J. Electrochem. Soc.* **137** 775

Groce F, Persi L, Scrosati B, Serraino-Fiory F, Plishta E and Hendrickson M A 2001 *Electrochim. Acta* **46** 2457

Jaipal Reddy M, Sreepathi Rao S, Laxmi Narasaiah E and Subba Rao U V 1995 *Solid State Ionics* **80** 93

Jonscher A K 1977 *Nature* **267** 673

Kumar B and Scanlon L G 1994 *J. Power Sources* **52** 261

Macdonald J R 1987 *Impedance spectroscopy, emphasizing solid materials and systems* (New York: Wiley)

Matsuo Y and Kuwano J 1995 *Solid State Ionics* **79** 295

Morita M, Fujisaki T, Yoshimoto N and Ishikawa M 2001 *Electrochim. Acta* **46** 1565

Munichandraiah N, Scanlon L G, Marsh R A, Kumar B and Sircar A K 1995 *J. Appl. Electrochem.* **25** 857

Peled E, Golodnitsky D, Ardel G and Eshkenazy V 1995 *Electrochim. Acta* **40** 2197

Plocharski J, Wieczorek W, Przyluski J and Such K 1989 *Appl. Phys.* **A49** 55

Polu A R and Kumar R 2011 *E-J. Chem.* **8** 347

Polu A R and Kumar R 2012 *E-J. Chem.* **9** 869

Polu A R and Kumar R 2013 *Internat. J. Polym. Mater.* **62** 76

Polu A R, Kumar R and Dehariya H 2012 *AIP Conf. Proc.* **1447** 969

Polu A R, Kumar R, Causin V and Neppalli R 2011 *J. Korean Phys. Soc.* **59** 114

Przyluski J, Sickierski M and Wieczorek W 1995 *Electrochim. Acta* **40** 2101

Przyluski J and Wieczorek W 1989 *Solid State Ionics* **36** 165

Rajendran S and Uma T 2000a *J. Power Sources* **88** 282

Rajendran S and Uma T 2000b *Mater. Lett.* **44** 208

Ramalingaiah S, Srinivas Reddy D, Jaipal Reddy M, Laxmi Narasaiah E and Subba Rao U V 1996 *Mater. Lett.* **29** 285

Robinson J L 1976 *The primary battery* Vol. II, (eds) N C Cahoon and G W Heise (New York: Wiley) p. 149

Sekhon S S and Sandhar G S 1998 *Eur. Poly. J.* **34** 435

Sreepathi Rao S, Jaipal Reddy M, Laxmi Narasaiah E and Subba Rao U V 1995 *Mater. Sci. Eng.* **B33** 173

Subba Reddy Ch V, Sharma A K and Narasimha Rao V V R 2004 *Ionics* **10** 142

Vijayakumar G, Karthick S N, Sathiya Priya A R, Ramalingam S and Subramania A J 2008 *Solid State Electrochem.* **12** 1135

Wagner J B and Wagner C J 1957 *Chem. Phys.* **26** 1597

Weston J E and Steele B C H 1982 *Solid State Ionics* **7** 75

Wieczorek W 1992 *Mater. Sci. Eng.* **B15** 108

Wieczorek W, Florjanczyk Z and Stevens J R 1995 *Electrochim. Acta* **40** 2251

Wieczorek W, Such K, Wycislik H and Plocharski J 1989 *Solid State Ionics* **36** 255